L80 Pipe Steel Microstructure Assessment Using Ultrasonic Testing

J.R. Kennedy, J.B. Wiskel, D.G. Ivey and H. Henein

Department of Chemical and Materials Engineering, University of Alberta, Edmonton, Canada T6G 1H9

Abstract

The potential exists to use ultrasonic shear velocity for real time microstructure assessment of the quenching step in the heat treatment of L80 steel pipe. L80 steel samples were austenitized and subsequently cooled in different quench mediums (water, oil, heated oil, air and furnace) to produce microstructures ranging from primarily martensite to coarse ferrite/pearlite mixed structures. Following heat treatment, the samples were ultrasonically tested, tensile and hardness tested and metallographically examined. The shear wave velocity was observed to increase as the underlying microstructure of each sample changed from primarily martensite, to primarily bainite and finally to coarse ferrite + pearlite. The measured shear wave velocity exhibited an inverse linear dependence on both yield strength and microhardness.

Keywords: ultrasonic testing, steel, L80, pipe, microstructure assessment, martensite, velocity, attenuation

1.0 Introduction

L80 is a low to medium carbon, heat treatable alloy steel used as casing pipe in the oil and gas industry [1]. Following pipe forming process, the L80 is austenitized, then quenched and tempered to the required mechanical properties (i.e., minimum yield strength of 80 ksi or 550 MPa). Ideally, the quenched L80 steel microstructure should be entirely martensite in order to achieve the strength requirements and ensure uniform properties throughout the steel for subsequent tempering operations and in the final pipe. Evaluation of the pipe properties and microstructure is typically undertaken only after the tempering process. An in-situ methodology to evaluate the quenching process (i.e., the ability of the quenching process to form martensite through the skelp thickness) is not currently available.

The potential, however, exists to assess the microstructure of quenched L80 steel using ultrasonic shear wave velocity. Freitas et al. [2] measured ultrasonic wave velocity in AISI 1045 steel that was austenitized and then either water quenched, oil quenched or normalized. A martensitic microstructure exhibited a lower shear velocity (≈ 3185 m/s) relative to a ferrite + pearlite microstructure. Gur et al. [3] measured the shear velocities of martensite, bainite, fine pearlite-ferrite and coarse pearlite-ferrite in AISI 4140 and 5140 steel. The martensitic microstructure exhibited a lower shear wave velocity (3196 – 3202 m/s) compared to a ferrite + pearlite microstructure. Papadakis [4] observed that the shear wave velocity in martensite (3195 m/s) for a SAE 4150 steel was lower than in either bainite (3236 m/s) or pearlite + ferrite (3252 m/s).

The work presented in this paper measures the ultrasonic shear velocity of laboratory austenitized and cooled L80 steel samples. The severity of cooling ranges from very high (water quenching) to very low (furnace cooling) to obtain a variety of microstructures ranging from primarily martensite (in the former) to coarse ferrite + pearlite (in the latter). The shear velocity of each heat treated sample is measured followed by hardness and tensile testing. Metallographic analysis was also undertaken to determine the general microstructure and grain size. The feasibility of using ultrasonic shear wave velocity testing for evaluation of the quenched L80 microstructure was assessed.

2.0 Background

The microstructures present in quenched L80 steel and their potential effect on both ultrasonic velocity and attenuation are discussed in this section. Calculated shear velocities for both isotropic and anisotropic steel with different microstructures is presented.

2.1 Microstructure of Quenched L80

The phases present in the quenched microstructure can include martensite (M), bainite (B), ferrite (F) or pearlite (P) [5]. Figure 1 is the CCT diagram [6] of a steel equivalent to L80, similar to that used in this study. For a cooling rate > 120 °C/s, a structure consisting of primarily martensite would form. For lower cooling rates, a mixture of phases (e.g., Martensite + Bainite or Ferrite + Pearlite, etc.) would form.

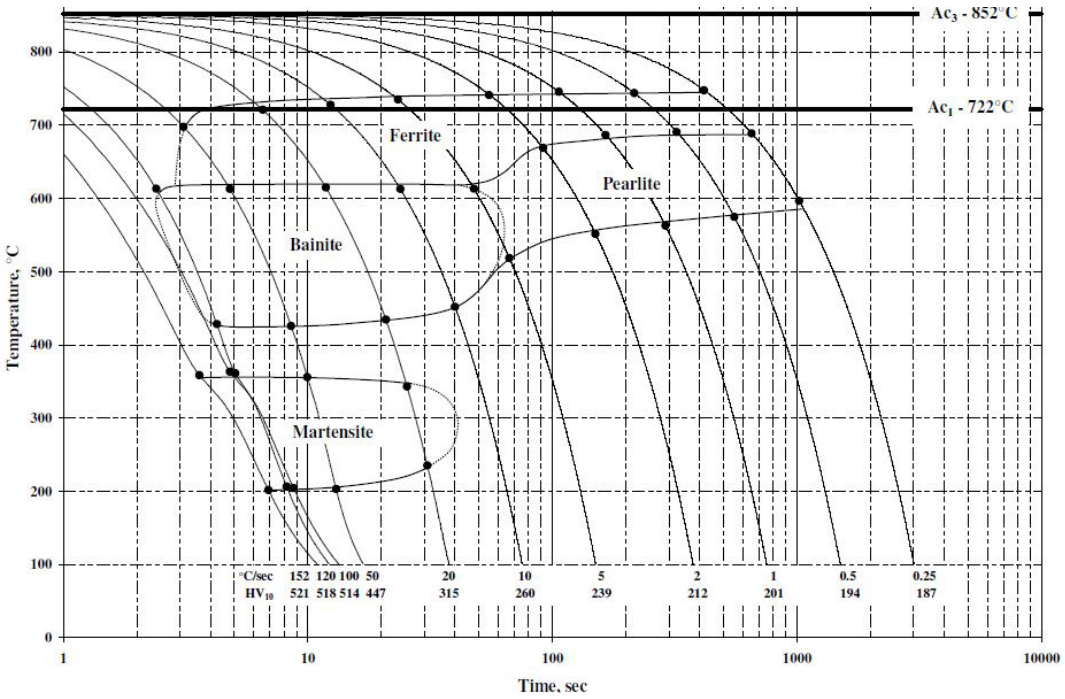

Figure 1: CCT diagram for a steel equivalent to L80 [5]

2.2 Ultrasonic Velocity in Steel

The velocity of an ultrasonic wave moving through L80 is dependent on both the crystal structure and the elastic properties associated with the crystal structure(s) present in the steel.

2.2.1 Elastic constants for ferrite and martensite

Table 1 gives the elastic constants (C_{11}, C_{12} and C_{44}), elastic modulus (E), density (ρ) and Poisson's ratio (v) for ferrite and the corresponding values experimentally determined for a 0.50 wt% C martensitic steel [7]. The elastic constants for the martensite a 0.5 wt% C martensite [7] show $C_{11} \approx C_{33}$, $C_{12} \approx C_{13}$ and $C_{44} \approx C_{66}$. The equivalency of each of these elastic constants is characteristic of a cubic structure [8]. Based on this equivalency, a cubic assumption for the martensite phase will be used in subsequent shear wave velocity calculations.

Table 1 - Elastic constants for ferrite and martensite [7]

Phase	C_{11} (GPa)	C_{12} (GPa)	C_{44} (GPa)	v	E (GPa)	ρ (kg/m^3)	A
Ferrite	232.0	135	116.0	0.289	211.9	7851	2.39
Martensite	268.1	111.2	79.1	0.292	203.5	7709	1.01

2.2.2 Elastic anisotropy

Elastic anisotropy in a crystalline structure is defined as a variation in elastic properties with direction. For phases exhibiting cubic symmetry, an anisotropy factor (A) can be calculated using the Zener ratio [9]:

$$A = \frac{2 \cdot C_{44}}{C_{11} - C_{12}} \tag{1}$$

where C_{11}, C_{12} and C_{44} are the elastic constants defined in Table 1. A = 1 defines an isotropic material, while A values >> 1 indicate an increasing degree of elastic anisotropy. The A values calculated for ferrite (2.39) and for martensite (1.01) are shown in Table 1. The relatively large value of A for ferrite indicates that the velocity of sound waves for this structure can be sensitive to ultrasonic testing orientation (depending on the severity of any crystallographic texture that may exist).

2.3 Ultrasonic velocity calculations

Ultrasonic shear wave velocities in a crystalline elastic medium can be calculated using two approaches: an isotropic approach and the Christoffel equation which is applicable to anisotropic materials.

2.3.1 Isotropic velocity

In its simplest form, the velocity of sound in a material can be approximated using the following equation [10]:

$$V_o = \sqrt{\frac{E}{\rho}} \tag{2}$$

where V_o is the generic velocity of sound, E is the Young's modulus and ρ is the density of the material. The shear velocity (V_{Si}) in an isotropic material can be calculated [11] using:

$$V_{Si} = V_o \cdot \sqrt{\frac{1}{2 \cdot (1+\nu)}} \tag{3}$$

where ν is the Poisson's ratio for the material.

2.3.2 Anisotropic velocity – Christoffel Equation

The ultrasonic velocities for an anisotropic material can be calculated using the Christoffel equation [11, 12]. The Christoffel equation in matrix form [8, 12] is as follows

$$\begin{bmatrix} \lambda_{11} - \rho V^2 & \lambda_{12} & \lambda_{13} \\ \lambda_{12} & \lambda_{22} - \rho V^2 & \lambda_{23} \\ \lambda_{13} & \lambda_{23} & \lambda_{33} - \rho V^2 \end{bmatrix} \cdot \begin{bmatrix} p_1 \\ p_2 \\ p_3 \end{bmatrix} = \begin{bmatrix} 0 \\ 0 \\ 0 \end{bmatrix} \tag{4}$$

where λ_{ij} are functions of C_{ij} - the elements of the stiffness tensor in the Voigt notation. The values of λ_{ij} are calculated from elastic constants (i.e., C_{11}, C_{12} and C_{44}) and the angle the ultrasonic wave makes with the x, y and z axes of the cubic crystal system [11-13]

The three (3) real roots of the determinant of Equation 4 are calculated and correspond to three ultrasonic velocities [14], two shear modes (V_{S1} and V_{S2}) and one longitudinal (or compression) mode (V_L). For an isotropic material V_{S1} and V_{S2} are identical. For an

anisotropic material a difference in elastic properties orthogonal to the shear wave propagation direction can result in differences between V_{S1} and V_{S2}.

Table 2 shows both the isotropic shear velocity (V_{Si}) and the anisotropic shear velocities calculated along the [100] and [110] unit cell directions for both ferrite and martensite [13]. The [100] and [110] crystal directions were arbitrarily taken to illustrate the effect of crystal orientation on shear velocity. The ferrite phase (high A value) shows shear velocities that are highly sensitive to propagation direction ([100] vs. [110]) with the velocity ranging from 4147 m/s to 2719 m/s. Conversely, martensite with a low A value (when approximated as a cubic structure) exhibits shear velocities that are relatively insensitive to propagation direction in the unit cell. For this work, V_{ST} will indicate a shear wave in which particle displacement is transverse to the rolling direction and V_{SP} will indicate a shear wave in which particle displacement is parallel to the rolling direction

Table 2 - Calculated isotropic and anisotropic shear velocities for ferrite and martensite

Phase	V_{Si} (m/s)	V_{S1} (m/s)		V_{S2} (m/s)	
		[100]	[110]	[100]	[110]
ferrite	3235	4147	2719	4147	4147
martensite	3196	3202	3194	3202	3202

2.4 Focus of study

The purpose of this work is to evaluate the potential of using ultrasonic testing to assess the microstructure of L80 immediately following the quenching step in the heat treatment. Ultrasonic shear velocities (parallel and perpendicular to the pipe length) were measured in L80 samples cooled from austenite at a variety of cooling rates. These shear velocities were correlated with the yield strength and hardness of the quenched samples and with the underlying microstructure. In addition, a ratio of measured shear velocities and a ratio of the longitudinal to shear velocities were also examined as a means of assessing the L80 steel microstructure without the need for precise pipe wall thickness measurements.

3.0 Materials and Experimental Methods

This section will describe the L80 steel used in this work, the heat treatments applied to the L80 samples and the metallographic analysis, tensile testing and ultrasonic testing undertaken on each heat treated sample.

3.1 L80 Steel

The composition of the L80 steel skelp (9 mm thick) is shown in Table 3. The moderate levels of carbon (C) and manganese (Mn) in addition to the small amount of chromium (Cr), give this steel moderate hardenability.

Table 3 - Composition of L80 steel

	Fe	C	Mn	Si	Cr	Mo	Nb+Ti+V
wt%	balance	0.24	0.99	0.20	0.16	0.01	0.032

Samples 240 mm long by 20 mm wide and 4 mm thick were machined from the ¼ through thickness position of the L80 skelp for heat treatment and subsequently ultrasonic testing, metallographic analysis, and hardness and tensile testing.

3.2 Heat Treatment

The L80 samples were heat treated in the as-received (uncoated) steel condition and in the coated condition. The coated samples were immersed in a ceramic mortar (and dried) prior to heat treatment [14]. The purpose of the coating was to extend the range of cooling rates (and microstructures) of the uncoated samples.

Each sample was individually austenitized in a box furnace to a temperature of 1000°C [14]. Following austenitizing, the uncoated samples were cooled differently including; a water quench (WC), an oil quench (OC), a quench in warm oil (heated to 200°C) (200), air cooling (AC) and furnace cooling (FC). Three (3) samples were tested for each cooling condition. The same cooling procedure was applied to the coated samples. The coated samples are labeled as CWC, COC, C200, CAC and CFC.

3.3 Metallographic analysis, and hardness and tensile testing

Following heat treating, the quenched samples were surface ground to a thickness of 3 mm to ensure both a consistent surface finish and parallel faces. A sample was sectioned from the near the end of the quenched bar, metallographically prepared and etched with 2% Nital. The phases present in each sample were qualitatively determined.

The grain size for each sample was measured using the circle intercept method [15]. For the ferrite + pearlite microstructure the grain size is an average of both the ferrite grain size and the pearlite colony size. For the martensitic and bainitic structures, the grain size value is indicative of the colony size and not the individual size of the laths for either structure.

Vickers hardness testing (HV_1) was then undertaken on the mounted sample. The remainder of the original austenitized and cooled sample was machined into an ASTM compliant rectangular tensile sample [16]. The yield stress for each tensile test was determined using the 0.02% offset method [17].

3.4 Ultrasonic evaluation

Ultrasonic testing was performed on each tensile bar (prior to tensile testing) at three locations along the tensile bar length. The ultrasonic tests were carried out using a Socomate USPC7100LA ultrasonic pulser/receiver with a desktop PC. The shear wave tests used a 10 MHz normal incidence shear wave transducer with an integral 6 mm delay block. Sonotech brand shear gel was used as the couplant. The shear wave tests were initially conducted with the transducer aligned with the rolling direction (atom motion parallel to the rolling direction) to measure the velocity (V_{SP}). The shear wave tests were then conducted with the transducer placed perpendicular to the rolling direction to measure the shear velocity (V_{ST}). Longitudinal wave tests used a 10 MHz normal incidence longitudinal wave transducer with synthetic SAE 5W30 oil as couplant. The wave velocities were calculated [14] using the time-of-flight between each reflection of the first eight sample backwall reflections and the sample thickness.

4.0 Results

The metallographic analysis is presented followed by the measured hardness and tensile test values. The measured ultrasonic velocities are then presented and correlated with yield strength and hardness.

4.1 Metallographic Analysis – Uncoated Samples

Metallographic images for the WC, OC, 200, AC and FC samples (taken from the mid-wall of each sample) are shown in Figure 2 a-e respectively. Similar microstructures were observed in the coated samples. The WC sample consists primarily of martensite (M) [18] with some regions of bainite (B) [19], as shown in Figure 2a. A similar dual phase structure is observed for the OC sample (Figure 2b). The 200 (heated oil quenched) sample also exhibits a martensite/bainite structure (Figure 2c), although qualitatively a larger fraction of the microstructure (relative to the WC and OC samples) is present as bainite. The AC and FC structures (Figure 2d and e, respectively) consist of ferrite and pearlite [20] with the FC sample qualitatively exhibiting a coarser structure.

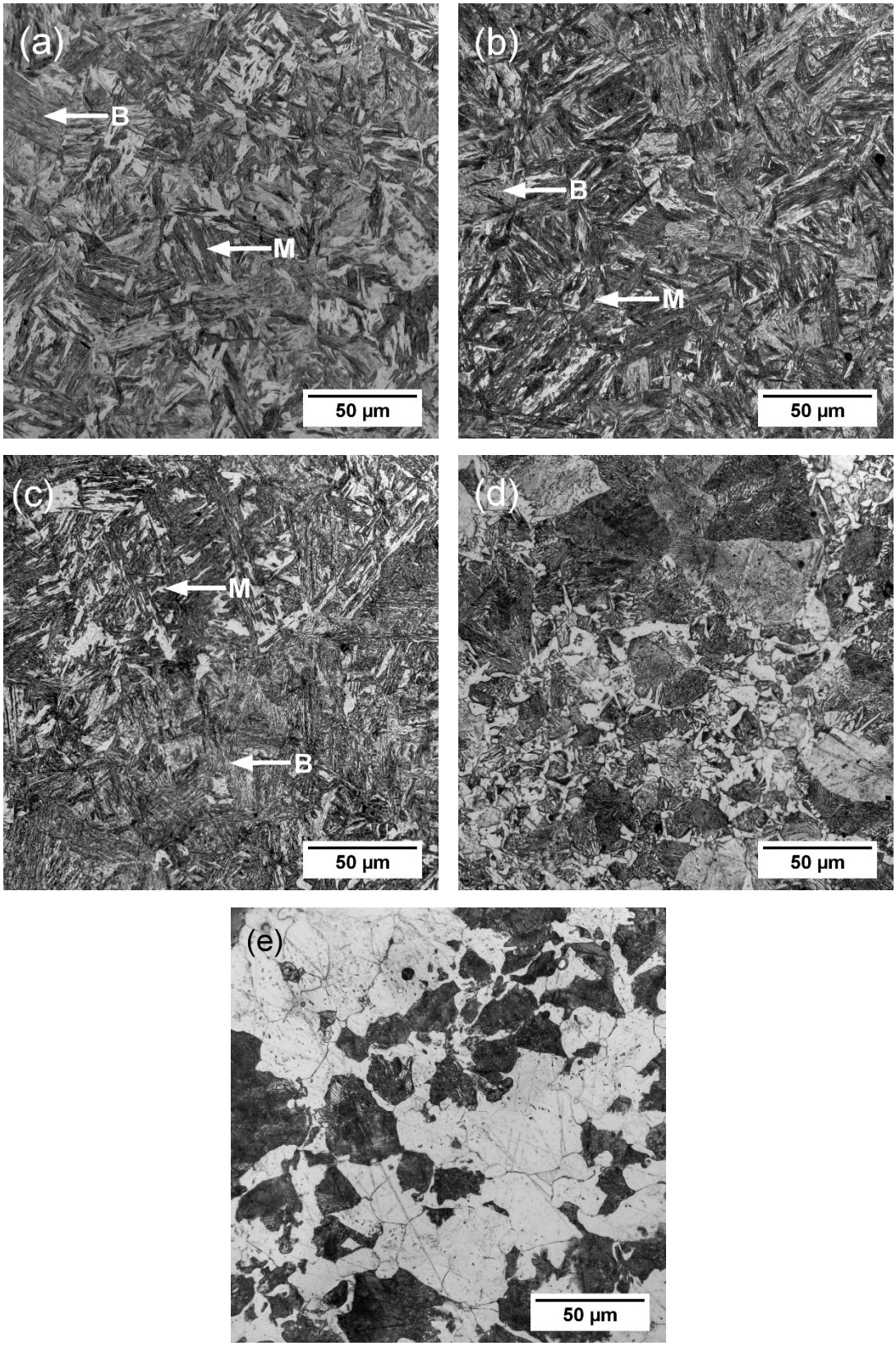

Figure 2: Representative bright field optical micrographs of samples (a) WC (b) OC (c) 200 (d) AC and (e) FC with example martensitic (M) and bainitic regions (B) marked.

The grain size measurements and predominant phases observed for each sample are summarized in Table 4. The phases identified in Figure 2 (Table 4) are consistent with the phases in Figure 1. At the higher cooling rates (120 - 152°C/s, estimated) martensite with some bainite is observed, while at the lowest cooling rates (0.25°C/s) the structure is primary ferrite and pearlite.

Table 4 - Measured grain/colony size and phases observed

Sample	Grain/Colony Size (μm)	Phases Observed
FC	72 ± 55*	Ferrite + Pearlite
AC	81 ± 44*	Ferrite + Pearlite
200	72 ± 10*	Bainite + Martensite
OC	81 ± 2*	Martensite + Bainite
WC	86 ± 28*	Martensite + Bainite

* one standard deviation.

4.2 Hardness Measurements

The average (minimum of thirty readings) Vickers hardness (HV_1) measured for each of the heat treatments are shown in Table 5. The highest hardness values (HV_1 = 515) are observed for the water quenched (WC) samples, similar to the hardness value for the highest cooling rates in Figure 1. The hardness for a completely martensitic structure (for a 0.24 wt% C steel) is $HV_1 \approx 500$ to 525 [21]. The oil quenched sample (OC) has a hardness ($HV_1 \approx 431$), which corresponds to a cooling rate of 50°C/s (Figure 1). The average hardness of the air cooled (AC) was HV_1 = 179 and the average hardness for the furnace cooled (FC) was HV_1 = 140.

4.3 Tensile Tests

Representative tensile curves from the WC, OC, 200, AC and FC samples are shown in Figure 3. The WC sample exhibits the highest strength followed by the OC, 200, AC and FC samples.

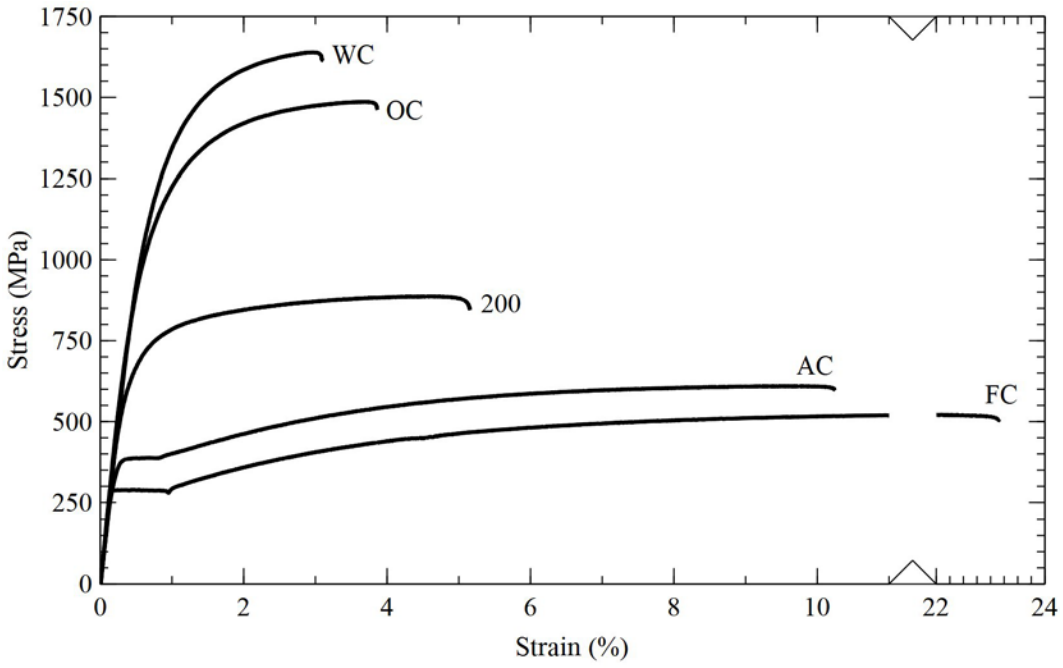

Figure 3: Representative tensile curves for WC, OC, 200, AC and FC samples

The yield strength (obtained using the 0.02% offset method) vs. hardness for both the uncoated and coated heat treated samples is shown in Figure 4. The uncoated samples (dark squares) exhibit an approximately linear relationship between yield strength and hardness with the highest yield strength corresponding to the highest hardness. The coated heat treated data points (lighter coloured circles) exhibit a similar relationship. However, two coated samples (dashed circled data points) show relatively low yield stress values at relatively high hardness values. This discrepancy may be attributed to non-uniformity of the coating along the sample length leading to variances in the cooling rate and structure.

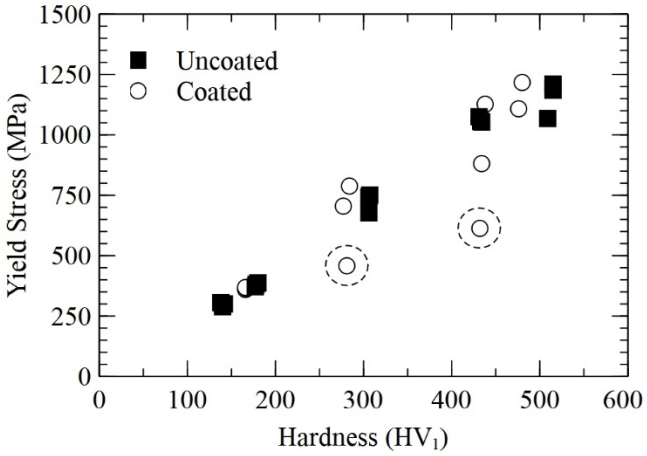

Figure 4: Yield strength vs HV_1 for both uncoated and coated heat treated samples. Dashed circles indicate non-uniform samples discarded from further analysis.

4.4 Ultrasonic Velocity Correlation with Yield Stress and Hardness

Figure 5 a and b show the measured mean value of V_{ST} (V_{SP} shows similar correlations) for each heat treated sample as a function of yield strength and hardness, respectively, the error indicated being one standard deviation in the spread of measurements taken. As yield stress and hardness decrease (i.e., a change in the underlying microstructure), the shear velocity V_{ST} increases. The approximate microstructures are indicated on each figure along with a horizontal dashed line representing the calculated isotropic shear velocity for martensite (V_{SMi} =3196 m/s). The measured value of V_{ST} approaches V_{SMi} at higher strengths and hardness values. The highest measured VST value (3202 m/s) compares reasonably well with literature values for 100% martensite (3196 – 3202 m/s [3] and 3195 m/s [4])

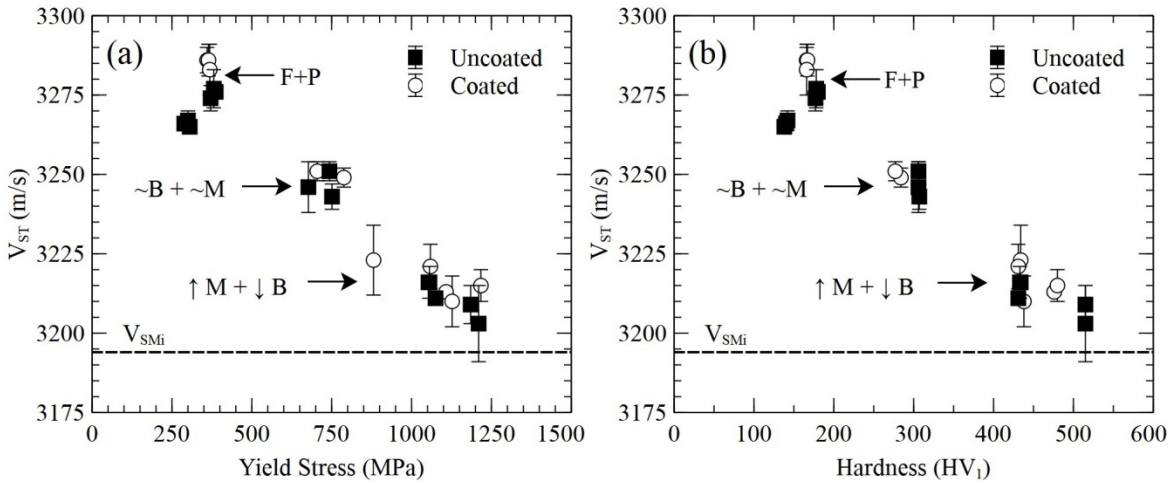

Figure 5: V_{ST} (a) as a function of yield strength and (b) as a function of Vickers Hardness

4.5 Comparison of V_{ST} and V_{SP} velocities

The shear velocity was taken with the atom motion either parallel (V_{SP}) or perpendicular (V_{ST}) to the hot rolling direction of the heat treated skelp. The values of V_{SP} and V_{ST} are compared in Figure 6. The dashed diagonal line represents equal values of V_{SP} and V_{ST}. For a completely isotropic microstructure, the measured shear velocity values (for both martensite and ferrite) should fall on this line. For the shear velocities associated with a predominantly martensitic structure, the value of V_{ST} is only slightly above the equivalency line. For the ferrite + pearlite microstructures, the value of V_{ST} is further above the isotropic line. In addition, the shear velocities for the ferrite + pearlite samples are larger than expected for isotropic ferrite (3235 m/s).

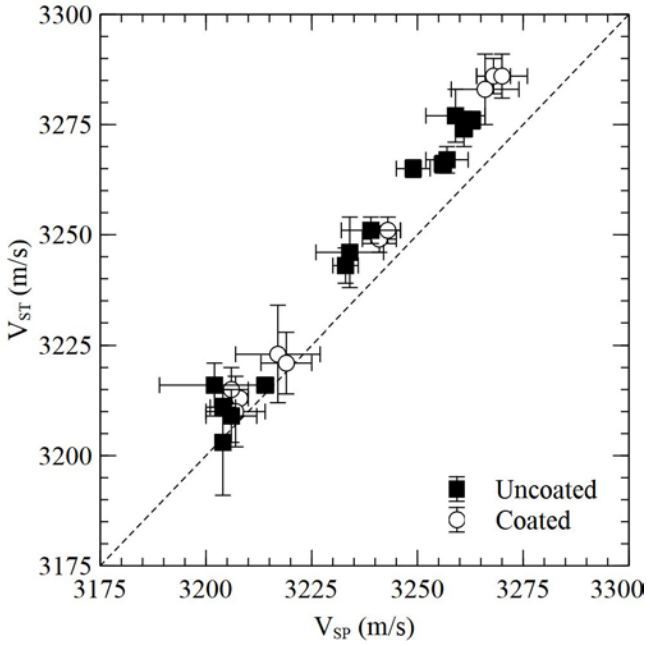

Figure 6: Comparison of measured shear velocities, V_{SP} and V_{ST}. The dashed line shows a 1:1 ratio between the velocities, indicating isotropy.

5.0 Discussion

This section discusses the effect of microstructure on ultrasonic velocity and the applicability of applying ultrasonic testing for microstructure analysis of the quenching process for L80 pipe. Three potential methods are presented, two based on the fundamental relationships between ultrasonic shear wave velocities and microstructure and a third empirical relation found between the ratio of shear/longitudinal velocity and microstructure.

5.1 Shear Velocity

The measured value of shear velocity (both transverse and parallel) for the water quenched heat treated L80 (3202 to 3209 m/s) are slightly higher than the theoretical value predicted for an isotropic martensitic structure (3196 m/s) as shown in Table 1. Metallographic assessment indicates that the water quenched samples are comprised of primarily martensite with some bainite. The measured shear velocity was observed to increase with decreasing yield stress/hardness and is associated with a decreasing amount of martensite in the WC, OC and 200 samples. The ferrite + pearlite microstructure in the AC and FC samples exhibit a significantly higher transverse shear velocity that in the martensite/bainite mixed structure. On the basis of these results shear wave velocity values provide a

reasonable assessment of the underlying microstructure particularly as the microstructure becomes less martensitic (i.e. more bainitic) or the microstructure becomes ferrite + pearlite. As this method differentiates between microstructures based solely on a single velocity, in order to evaluate the microstructure an accurate measurement of the sample thickness is required.

5.2 Non-equivalency of Transverse and Parallel Shear Velocities

The transverse (V_{ST}) and parallel shear velocities (V_{SP}) measured in this work for the heat treated samples were not equivalent to each other. Figure 7 shows the ratio of V_{ST}/V_{SP} as a function of yield strength. Since this is a ratio of two velocities over the same distance (the sample thickness) it is equivalent to the ratio of the travel time (time of flight) for shear waves with displacement directions parallel and transverse to the rolling direction, as such it is both dimensionless and does not require an accurate measurement of the sample thickness. As the yield strength decreases (the amount of ferrite increases either in the bainite or ferrite + pearlite microstructures), the V_{ST}/V_{SP} ratio increases (i.e., a greater deviation from the equivalency line shown in Figure 6). This change in the ratio suggests that an inherited texture in the heat treated sample may be influencing the measured velocity values. Depending on the amount of residual texture following austenitization of the hot rolled sample, specific orientations can potentially lead to a variation in transverse and parallel shear velocities [22]. The relatively small difference between the shear velocities for a primarily martensitic structure (i.e., high yield strength) is consistent with the low anisotropy factor (A) for martensite. The difference between V_{ST} and V_{SP} increases as the underlying structure (yield strength and hardness as well) changes from predominantly martensite to more bainite and ultimately ferrite + pearlite. The anisotropy factor for ferrite (present in bainite and ferrite + pearlite) is relatively large; hence, a larger difference between V_{ST} and V_{SP} may exist (see Table 2) due to texture in the underlying structure. Therefore, in addition to using absolute shear velocity as a measure of the underlying microstructure, an increase in the V_{ST}/V_{SP} ratio can be used as an indication of decreasing martensite fraction in the quenched L80 steel.

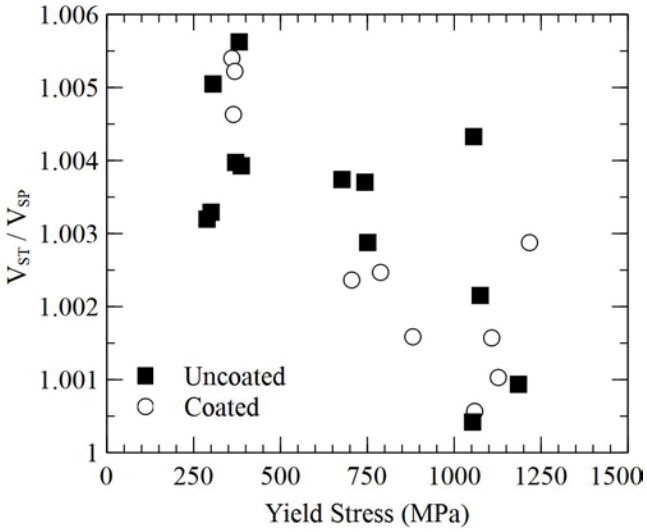

Figure 7: V_{ST}/V_{SP} ratio as a function of yield strength

5.3 Empirical Method using both Shear and Longitudinal Velocities

A further emperical method was also developed using beth shear and logitudinal velocities. As shown in Figure 8 the longitudinal velocities of the samples do not correlate well with the yield strength, nor the microstructures of the samples. It has been found empirically however that the ratio of the longitudinal velocity to shear velocity does correlate with the yield stress and thus microstructure. For ease of understanding the V_L/V_{SP} ratio is shown in Figure 8, similar behiour is also seen with the V_L/V_{ST} ratio. As with the V_{ST}/V_{SP} ratio this is a dimensionless method which does not require knowledge of the sample thickness as only the time between backwall reflections for each wave is needed. While the previous two methods are based on the fundamental relationship between shear wave velocity and the elastic constants of differing microstructures, this method relies on the longitudinal velocities being insensitive to microstructure and acting as a benchmark to which the shear wave velocities are compared so accurate measurement of the sample thickness is not required. Fundamentally the longitudinal velocities should vary with microstructure [3] however experimentally it has been found to be less sensitive to changes than shear waves [23], as was the case in this study (Figure 8). Care must then be taken if this method is used to note the longitudinal values as inconsistent values may result in erroneous evaluation of the microstructure.

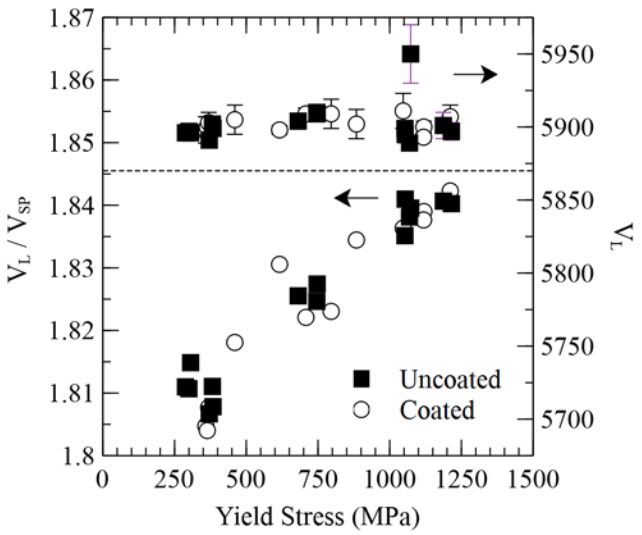

Figure 8: Longitudinal velocity (V_L) and V_L/V_{SP} ratio as a function of yield strength

5.4 Application of Ultrasonic Testing to Evaluation of Quenched L80 Microstructure

The testing and results provided in this work indicate that ultrasonic shear velocity measurements can be used to track the variation of martensite in heat treated L80 steel. In addition, the potential exists to use the V_{ST}/V_{SP} ratio as a measure of the fraction of martensite present. For samples in which some texture is inherited from the hot rolled skelp, a higher V_{ST}/V_{SP} ratio may be an indicator of increased amounts of ferrite. A further empirical relation was also found which may be used to identify microstructure based on the $V_L/V_{S(T\ or\ P)}$ ratio.

6.0 Conclusions

1] The measured shear velocity (3204 - 3208 m/s) values for a water quenched L80 steel, with a predominantly martensitic structure, show reasonable agreement with both a theoretical shear velocity value for martensite and with measured literature shear velocity values for martensite.

2] Both the transverse and parallel shear velocities increased with decreasing yield strength and hardness which is attributed to a change in microstructure from predominantly martensite to bainite and subsequently ferrite + pearlite.

3] The ratio of transverse shear velocity to parallel shear velocity (V_{ST}/V_{SP}) increased with decreasing yield strength. The difference is attributed to residual texture and the higher anisotropy factor (A) for the ferrite phase relative to martensite.

4] The trends in velocity values with different cooling severity indicates that the potential exists to use ultrasonic information (i.e., shear velocity and/or ratio of V_{ST}/V_{SP}) to assess the microstructure of a quenched L80 steel.

Acknowledgements

The authors wish to acknowledge the support of EVRAZ N.A. Inc. TCPL and NSERC of Canada for funding for this project.

Declaration of Interest

No potential conflict of interest was reported by the authours.

References

[1] API Specification 5-CT, Specification for Casing and Tubing, 9th Edition, June 2011

[2] V. Freitas, V. Alburquerque, E Silva , A. Silva and J. Tavarares, "Nondestructive characterization of microstructures and determination of elastic properties in plain carbon steel using ultrasonic measurements," Materials Science and Engineering A, 2010, vol. 527, pp. 4431-4437,

[3] C.H. Gur and B. O. Tuncer, "Characterization of microstructural phases of steels," Materials Characterization, 2005, vol. 55, pp. 160-166.

[4] E. Papakadis, 'Ultrasonic attenuation and velocity in three transformation products in steel", J. Appl. Phy., 1964, 35, pp. 1474-1482.

[5] V. Palanisamy, J.K. Solberg, B. Salberg and P.T. Moe, "Microstructure and Mechanical properties of API 5CT L80 casing grade steel quenched from different temperatures., OMAE2012, July 1-6, Rio de Janerio, ASME, 2012.

[6] IPSCO Research Report, Development of CCT Diagram, API 5CT Grade L80, Project 226-06, 2006

[7] S. Kim and W. Johnson, 'Elastic constants and internal friction of martensite steel, ferritic-pearlitic steel and α-iron' Mat. Sci. Eng. A, 2007, 452-453, pp. 633-639.

[8] B. Castagnede, W.Sachse and M. Thompson, 'Determination of the elastic constants of anisotropic materials via laser-generated ultrasound', Ultra. Int., 1989, pp.71-79.

[9] C. M. Kube, "Elastic anisotropy of crystals", Advances in Physics, 2016, 6, 095209.

[10] P. Laugier, G. Haiat, "Ch. 2: Introduction to the physics of ultrasound" in Bone Quantitative Ultrasound, Springer, 2011

[11] C. Lane, The Development of a 2D Ultrasonic Array Inspection for Single Crystal Turbine Blades, Springer Publishing, 2014, pp.13-39.

[12] J. Rose, Ultrasonic Waves in Solid Media, Cambridge University Press, 1999.

[13] J.B. Wiskel, J. Kennedy, D.G. Ivey and H. Henein, "Ultrasonic Velocity Evaluation of Three Grades of Heat Treated Steel", Cdn. Inst NDE Conf,, Edmonton, Canada, 2015.

[14] J. Kennedy, "Ultrasonic Evaluation of Microstructure in Pipe Steels", M.Sc. Thesis, University of Alberta, Canada, 2015.

[15] ASTM, E112-13, Standard Test Methods for Determining Average Grain Size, 2013.

[16] ASTM, E8m-04, Standard Test Method for Tensile Testing Metallic Materials, 2008

[17] C. Ross, “Mechanics of Solids” Elsevier Science, 1999.

[18] A.R. Marder G. Krauss, "The Morphology of Martensite in Iron Alloys," *Metallurgical Transactions,* vol. 2, pp. 2343-2357, 1971

[19] A.O. Benscoter B.L. Bramfitt, "Ch. 2 Origin of Microstructure," in *Metallographers Guide: Practice and Procedures for Irons and Steels*.: ASM International, 2001, pp. 23-48.

[20] B.L. Bramfitt, "Effects of composition, procesing and structure on properties of iron and steels," in *ASM Handbook Vol. 20: Materials Selection and Design*.: ASM International, 1997, pp. 357-382

[21] R.A. Grange, C.R. Hirbal and L.F. Porter, “Hardness of Tempered Martensite in Carbon and Low-Alloy Steels”, Met. Trans. A, 1977, Vol. 8a, pp. 1775-1785.

[22] A. Kaijalainen, P. Suikkanen and D.A. Porter, “Effect of re-austenitization on the transformation texture inheritance, IOP Conf. Series: Material Science and Engineering, 2015, 82, pp. 1-5.

[23] V. Rajendran, T. Jayakumar, P. Palanichamy, P S.M. Kumaran, "First Differential of temperature dependent ultrasonic parameters as an effecive tool for identifying precipitation reactions in a slow heat-treated 8090 Al-Li alloy," Journal of Alloys and compounds, vol. 464, pp. 150-156, 2008